

# Yielding and large deviations in micellar gels: a model

**Saroj Kumar Nandi**

Centre for Condensed Matter Theory, Department of Physics, Indian Institute of Science, Bangalore 560012, India

E-mail: [snandi@physics.iisc.ernet.in](mailto:snandi@physics.iisc.ernet.in)

**Bulbul Chakraborty**

Martin Fisher School of Physics, Brandeis University, Mail Stop 057, Waltham, Massachusetts 02454-9110, USA

E-mail: [bulbul@brandeis.edu](mailto:bulbul@brandeis.edu)

**A. K. Sood**

Department of Physics, Indian Institute of Science, Bangalore 560012, India

E-mail: [asood@physics.iisc.ernet.in](mailto:asood@physics.iisc.ernet.in)

**Sriram Ramaswamy**<sup>1</sup>

Centre for Condensed Matter Theory, Department of Physics, Indian Institute of Science, Bangalore 560012, India

E-mail: [sriram@tifrh.res.in](mailto:sriram@tifrh.res.in)

<sup>1</sup>On leave at TIFR Centre for Interdisciplinary Sciences, 21 Brundavan Colony, Narsingi, Hyderabad 500 075, India

**Abstract.** We present a simple model to account for the rheological behavior observed in recent experiments on micellar gels. The model combines attachment-detachment kinetics with stretching due to shear, and shows well-defined jammed and flowing states. The large deviation function (LDF) for the coarse-grained velocity becomes increasingly non-quadratic (and the probability distribution function non-Gaussian) as the applied force  $F$  is increased, in a range near the yield threshold. The power fluctuations are found to obey a steady-state fluctuation relation (FR) at small  $F$ . However, the FR is violated when  $F$  is near the transition from the flowing to the jammed state although the LDF still exists; the antisymmetric part of the LDF is found to be nonlinear in its argument. Our approach suggests that large fluctuations and motion in a direction opposite to an imposed force are likely to occur in a wider class of systems near yielding.

*Keywords:* Large deviations in nonequilibrium systems, Jamming and Packing, Rheology and transport properties, Fluctuations (theory)

Fluctuation relations (FR) as originally formulated [1, 2, 3, 4, 5, 6, 7] are exact statements connecting the relative probabilities of observing the production and the consumption of entropy at a given rate in a driven *thermal* system, and can be expressed as symmetry properties of the large-deviation function of the entropy production rate. An observable  $X_\tau$ , for example, the average power delivered over a time interval  $\tau$  is said to have the large-deviation property if its probability density decreases exponentially for large  $\tau$ ,  $\text{Prob}(X_{\tau \rightarrow \infty} = a) \sim \exp[-\tau \mathcal{W}(a)]$ . The decay rate  $\mathcal{W}$  is called the large-deviation function (LDF), and its behaviour for large  $a$  encodes information about the statistics of extremes of the underlying random process [8, 9]. The steady-state fluctuation relation [2, 3] states that  $\mathcal{W}(a) - \mathcal{W}(-a) \propto a$ .

In this paper we study numerically in some detail the large-deviation behaviour of a model for a macroscopic degree of freedom driven through a medium of dynamic attachment points. The model is motivated by precision creep rheometry studies [10] of a micellar gel at controlled stresses below its nominal yield point, that revealed that the small positive mean shear-rate, i.e., in the direction favoured by the imposed stress, was composed of a highly irregular time-series of positive and negative shearing events. Moreover the shear-rate fluctuations, which at constant stress are also power fluctuations, obeyed [10] a fluctuation relation of the Gallavotti-Cohen type [2, 3]. The measurements reported were made on a macroscopic degree of freedom, the angular position of the rheometer plate, which could not be influenced perceptibly by thermal noise. Fluctuations in this system must be a consequence of the imposed drive. The probability distribution of the angular-velocity fluctuations was found to be strongly non-Gaussian at large imposed stress. An effective temperature extracted from a comparison to the Gallavotti-Cohen relation was found to increase with the applied stress.

Our theoretical model reproduces the findings of the experiment but also finds departures from the fluctuation relation in the strict sense, in a certain parameter range, despite the existence of LDF. That is, it finds that the antisymmetric part of the LDF departs from linearity in its argument. Moreover, the model we present should apply to a wider class physical problems involving yield or escape in the presence of fluctuations. We shall return to these points at the end of the paper.

Consider an external force acting on some coordinate of a *thermal* system with inverse temperature  $\beta$ , and let the random variable  $w_t$  be the instantaneous rate of doing work in a given realization of the dynamics. Define

$$W_\tau = \frac{1}{\tau} \int_0^\tau w_t dt \quad (1)$$

to be the rate of doing work, binned or averaged over a time scale  $\tau$ . The steady-state fluctuation relation (FR) [11, 12] tells us

$$\frac{1}{\tau} \ln \frac{P(W_\tau)}{P(-W_\tau)} \asymp \beta W_\tau, \quad \tau \rightarrow \infty \quad (2)$$

where  $P(W_\tau)$  is the probability distribution function (PDF) of  $W_\tau$ , and  $\asymp$  denotes asymptotic equality. Underlying (2) is a more general relation, the existence of the

large deviation function (LDF) [8]. The principle of large deviation consists in the existence of the limit

$$\lim_{\tau \rightarrow \infty} -\frac{1}{\tau} \ln P(W_\tau) = \mathcal{W}, \quad (3)$$

where the limiting quantity  $\mathcal{W}$  is called the rate function or large-deviation function (LDF). Eq. 2 is then a statement about a symmetry property of the LDF, *viz.*, that its antisymmetric part is linear in its argument. A large class of experimental [13, 14, 15] and simulation [16, 17] results and theoretical calculations [18, 19, 20, 21] confirm the existence of relations of the FR type even in systems driven far away from equilibrium. Note that some of these systems are not obviously characterized by a thermodynamic temperature. In such cases the existence of a relation like (2) offers one way of defining an effective temperature [22].

The exact linearity in  $W_\tau$  as required by (2) is a strong restriction for a non-Gaussian random variable. Naturally there are situations [23, 24, 25, 26] where it does not hold. In the example of [23, 24], however, the large-deviation property itself does not hold. In our simple model, by contrast, the conventional FR fails to hold in some regions of parameter space even though the LDF exists. The model has the additional virtue of being constructed to model a physical situation, rather than as a mathematical counterexample, and will therefore be of wide interest.

Here are the main results of this work: (1) the model shows a sharp crossover from a creeping jammed state to steady flow (Fig. 2); (2) deep in the jammed state, the velocity fluctuations are Gaussian and obey the FR (Fig. 3); (3) near the threshold to free flow, the velocity fluctuations become non-Gaussian, but still obey the FR (Fig. 5); all these findings are in conformity with experiments [10]. (4) Just below the threshold, the velocity fluctuations are non-Gaussian and they don't obey FR, even though the LDF exists as is shown in Fig. 4). (5) If we keep the number of attachment points fixed, the effective temperature ( $T_{eff}$ ) decreases with increasing applied force ( $F$ ) in contrast to what is found in the experiment. To produce the correct  $T_{eff}$  vs  $F$  trend, we must allow the number of attachment points to increase with increasing  $F$  (Fig. 7).

The paper is organised as follows: in Sec 1 we present our model and we discuss the mean-field version of the model in Sec. 2. We present details of our exploration of parameter space and the results in Sec. 3 and conclude the paper with a discussion in Sec. 4.

## 1. The model

The micellar gel sample in the experiment is taken in a rheometer with a cone-plate geometry to ensure uniform strain rate through-out the sample, and the upper plate is rotated with a constant torque while keeping the lower plate fixed. The detailed geometry of the rheometer, however, is not important for the observed findings. We model the micellar gel medium as a collection of springs that are stretched by the applied torque when they are attached to the plates, and can detach when stretched by

a high enough force. We do not associate the “springs” with individual molecules or micelles but rather with adhering, deformable domains in the material, whose size we do not know. We assume the springs always remain attached to the stationary plate.

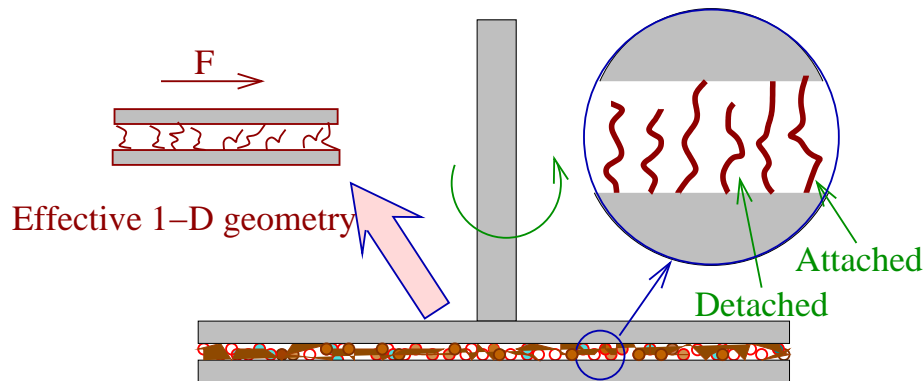


**Figure 1.** A schematic illustration of the model. The “springs” (see text) can get attached to or detached from the upper plate. The experimental geometry can be thought of as effectively one-dimensional with the force being applied in a particular direction.

We use an effective one-dimensional description in which  $X(t)$  is the total (angular) displacement of the upper plate as in Fig. 1 and let  $V(t) = dX(t)/dt$  be its instantaneous velocity. Let us consider  $f_i(t) = k_i x_i$  be the force on the  $i$ th spring at time  $t$  where  $k_i$  and  $x_i$  are respectively the spring constant and the extension of the spring. Then the spring will pull the plate backwards only if it is attached with the plate. Thus, we can write down the equation of motion for the upper plate as

$$M \frac{dV(t)}{dt} + BV(t) = F - \sum_i s_i f_i(t), \quad (4)$$

where  $M$  is the mass of the plate,  $B$  a viscous damping coefficient,  $F$  the force (actually torque) on the rheometer plates and  $s_i$  is a two state variable which can take on values 0 or 1. If  $s_i = 1$ , then the  $i$ th spring is attached with the plate and it is detached otherwise. Note that we have not specified the number  $N$  of “springs” in the model. It is not clear how to do this in the absence of a detailed microscopic theory. It is entirely possible that  $N$  depends on the imposed torque, or even that it is determined dynamically. We will assume it is a parameter of the system, and show the behavior in the  $N - F$  plane.

Now, if the spring is attached to the plate, it will stretch with the velocity of the plate; if it is detached it will relax. Thus

$$\frac{dx_i(t)}{dt} = -(1 - s_i)\gamma k_i x_i(t) + s_i V(t) \quad (5)$$

where  $\gamma$  is a kinetic coefficient. Thus,

$$\frac{df_i(t)}{dt} = -(1 - s_i)\gamma k_i f_i(t) + s_i k_i V(t). \quad (6)$$

Assume for simplicity that all  $k_i$ 's are equal, define  $\gamma k_i \equiv 1/\tau$ , redefine  $k_i V \rightarrow V$  in Eq. (6) and  $B/k_i \rightarrow B$  in Eq. (4). Ignoring inertia, we then obtain equations for  $V$  and  $f_i(t)$ :

$$BV(t) = F - \sum_i s_i f_i(t) \quad (7)$$

$$\frac{df_i(t)}{dt} = -(1 - s_i)f_i(t)/\tau + s_i V(t). \quad (8)$$

One could imagine more complicated modes of relaxation, for example the springs can partly redistribute forces among themselves. But Eq. (8) is the simplest possible model that contains the dominant mechanism. We will discuss the effect of a diffusive term later.

The state variables  $s_i$  are assumed to follow a stochastic dynamics. Let  $P_i(t) \equiv \text{Prob}(s_i = 1, t)$  be the probability that the  $i$ th spring is attached at time  $t$ . Then

$$\frac{dP_i(t)}{dt} = -W_D P_i(t) + W_A(1 - P_i(t)), \quad (9)$$

where  $W_A$  and  $W_D$  are the attachment and detachment rates, the most important input parameters of the model. It is possible to engineer these rates to reproduce different behaviours by the model. The feature that is essential to get negative fluctuations is that a spring with a large force on it gets reattached and pulls the plate in the opposite direction.

The fluid is a highly viscous glassy material and we can safely ignore the inertia term in Eq. (4). For notational convenience we set  $B$  to unity so that  $V = F - \sum_i s_i f_i$ . For a suitable choice of parameter values, as will be shown below, the model shows a jammed-flowing transition. This is not a true phase transition, but a strong crossover from slow creep to free flow.

## 2. The mean field calculation

In the mean field approximation, we assume the forces on all springs are the same and that they take some mean value in the steady state, as do the state variables ( $s_i$ ). In this approximation,  $\langle f_i \rangle = f$  and  $\langle s_i \rangle = s$  so that

$$\langle V \rangle = F - \sum_i \langle f_i s_i \rangle \simeq F - \sum_i \langle f_i \rangle \langle s_i \rangle = F - N s f, \quad (10)$$

where  $N$  is the total number of springs. In the steady state, (8) will yield

$$(1 - s)f/\tau = s\langle V \rangle \Rightarrow f = \tau s \langle V \rangle / (1 - s). \quad (11)$$

Using the above relation in Eq. (10), we find the velocity

$$\langle V \rangle = \frac{(1 - s)F}{(1 - s) + N s^2 \tau}. \quad (12)$$

In two extreme limits, if  $s = 1$ ,  $\langle V \rangle = 0$  and if  $s = 0$ ,  $\langle V \rangle = F$ . In the steady state,  $dP_i(t)/dt = 0$  so that

$$P_i = \frac{W_A}{W_A + W_D}. \quad (13)$$

Therefore, the steady state value of  $s$ , within the mean-field approximation, will be

$$s = \langle s_i \rangle = \sum_{s_i=0,1} s_i P_i = P_i = \frac{W_A}{W_A + W_D}. \quad (14)$$

The mean force on each spring becomes

$$f = \frac{\tau s F}{(1 - s) + N s^2 \tau}. \quad (15)$$

Thus, we see that  $\langle V \rangle$  depends on three time scales. To simplify the discussion, we fix  $\tau$  and  $W_A$  and take  $W_D/W_A$  to have an activated form. We recall that the mechanism of having a negative velocity (in the direction opposite to  $F$ ) events is that a spring with a large force on it gets reattached to the plate before it has completely relaxed its force. This can happen if the force relaxation is much slower than the attachment-detachment kinetics of the springs. Thus, to have a large number of negative events, we must have  $\tau W_A \gg 1$ . To ensure this, we chose the parameters as follows:  $\tau = 2.5$ ,  $W_A = 100$  and  $W_D = W_A e^{\alpha(f_i - f_0)}$ , with  $\alpha = 2.0$  and  $f_0 = 1.0$ . The springs can get attached with the plate at a constant rate irrespective of the force on it. But if it is already attached to the plate, it is more probable to get detached as the force on the spring increases. We have introduced the parameter  $\alpha$  to obtain a reasonably sharp transition from jammed to flowing state, at a force whose value is controlled by  $f_0$ . Restricting the form of  $W_D$  allows us to worry about one less parameter of the model. The predictions of mean-field version of the model are shown with solid lines in Fig. 2.

The activated nature of the attachment-detachment is reminiscent of rheology models with traps such as the SGR [27, 28, 29]. An essential difference between our model and the trap models [27, 28] is that the springs in our model retain the forces on them even after getting detached from the plate whereas the strain on a spring in the trap model becomes zero after it comes out of a trap. The simplest trap models can not show negative velocity events.

### 3. Details of the simulation and the results

We simulate the equations (7)-(9), setting  $B = 1$ , through the kinetic Monte-Carlo (KMC) method [30] to obtain the behaviour of our model. The advantage of KMC over the conventional Monte-Carlo method is that the time scale of the dynamics is entirely determined by the various rates of the problem. As we have discussed in the previous section, the various parameters of the model were chosen using the mean-field analysis to locate a regime in which a clear transition from jammed to flowing was seen, and adjusting rates to allow for significant negative velocity fluctuations.

The model shows a well-defined jammed to flowing transition that becomes sharper as we increase the number of springs  $N$  as is shown in Fig. 2 where the symbols are the

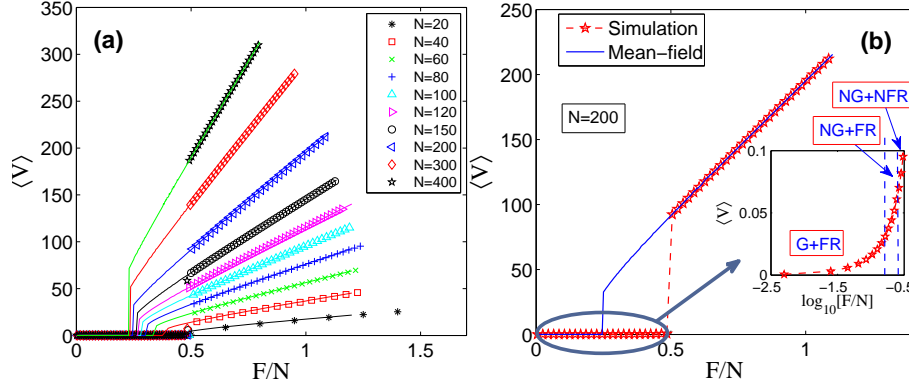


**Figure 2.** (a) The flow curves obtained from the simulation for various number  $N$  of springs with a particular set of parameter values (see text), the lines are the corresponding mean-field solution. (b) The flow curve is shown for  $N = 200$  for clarity. The mean-field solution overestimates the threshold. The regions are roughly marked based on whether the fluctuations are Gaussian (G) or non-Gaussian (NG) and whether they do obey the conventional FR or not.

simulation values and the corresponding curves are the mean-field solution. In Fig. 2(b) we show the flow curve for  $N = 200$  and the inset shows the behaviour in the jammed state in a semi-log plot where it is evident that even in the jammed state, the velocity is actually non-zero. The mean-field solution overestimates the threshold but agrees well with simulation results away from the transition.

In the jammed state, there is a significant number of negative velocity events, however, there are none once the system goes to the flowing state. To understand the fluctuations in the jammed state and test the regime of validity of the FR, we keep  $N = 200$  fixed, and find a threshold force  $F = 97.0$ . We take a value of the external force  $F = 20.0$  deep in the jammed state. From the instantaneous velocity as shown in Fig. 3 (a), we see that there is a significant number of negative velocity events. Since the applied force is constant, the statistics of velocity and power fluctuations are the same. We denote the velocity (or power) fluctuations with respect to the mean, averaged over a time interval  $\tau$  by  $W_\tau$ :

$$W_\tau = \frac{1}{\tau} \int_T^{T+\tau} \frac{V(t)}{\langle V \rangle} dt, \quad (16)$$

where the initial time  $T$  is arbitrary but taken in such a way that the difference between two consecutive  $T$  is greater than the mean correlation time of velocity. The PDF of  $W_\tau$  is shown in Fig. 3(b). The overlap of curves in the scaled plot [Fig. 3(c)] is evidence of the existence of the large-deviation function for the velocity. The nature of the distribution is determined by two parameters, Skewness ( $S$ ) and Kurtosis ( $K$ ):

$$S = \langle \delta W_\tau \rangle^3 / \sigma^3 \quad \text{and} \quad K = \langle \delta W_\tau \rangle^4 / \sigma^4 - 3, \quad (17)$$

where  $\delta W_\tau = W_\tau - \langle W_\tau \rangle$  and  $\sigma^2 = \langle \delta W_\tau^2 \rangle$ .  $S$  and  $K$  are defined so as to be zero for a Gaussian process and Fig. 3(d) shows that the distribution is Gaussian. Also,  $W_\tau$  obeys



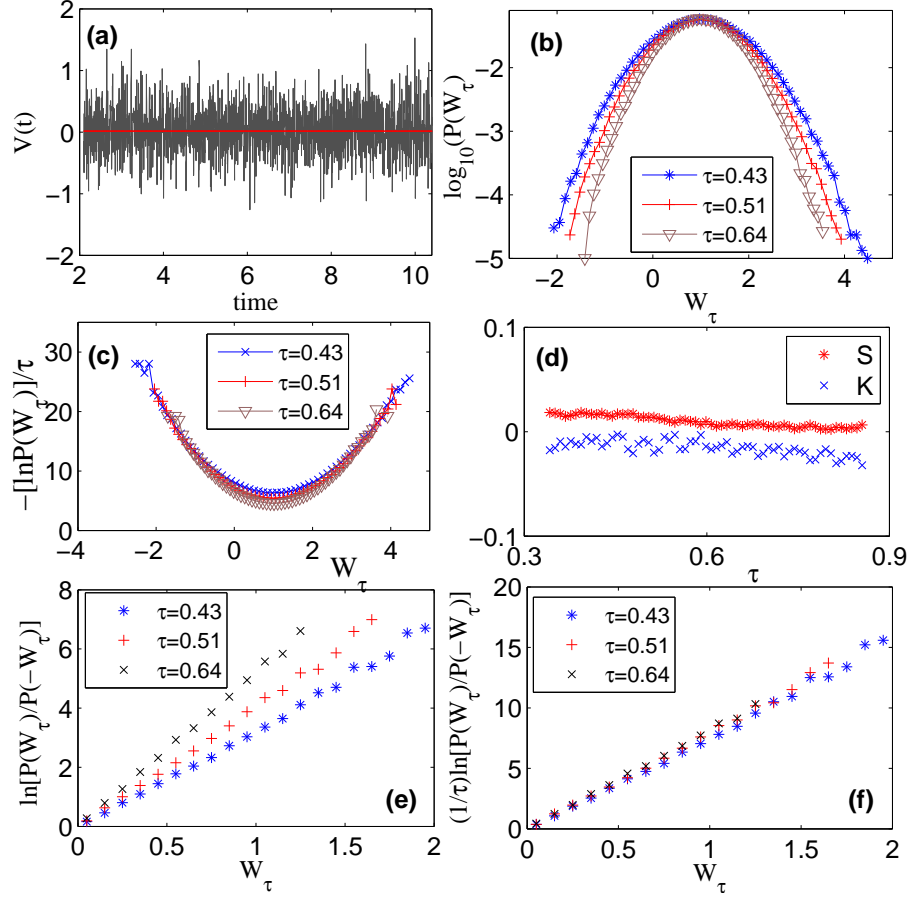


**Figure 3.** The behaviour of the model for the particular set of parameter values as specified in the text with  $N = 200$  and  $F = 20.0$  (a) The instantaneous velocity as a function of time, the thick line denotes the average velocity. There are a significant number of negative velocity events. (b) The probability distribution function (PDF) of the scaled coarse-grained velocity or work fluctuation (both are same since the applied force is constant)  $W_\tau$ . (c) The large-deviation function (LDF) for  $W_\tau$ . (d) The skewness ( $S$ ) and Kurtosis ( $K$ ) for velocity fluctuation are very small implying the PDF is Gaussian. (e)  $\ln[P(W_\tau)/P(-W_\tau)]$  vs  $W_\tau$  for various  $\tau$ . (f)  $(1/\tau)\ln[P(W_\tau)/P(-W_\tau)]$  vs  $W_\tau$  for various  $\tau$  collapse to a master curve that is straight line signifies that the velocity fluctuation obeys fluctuation relation.

the fluctuation relation as is evident from the plot of  $\ln[P(W_\tau)/P(-W_\tau)]/\tau$  vs  $W_\tau$  for various  $\tau$  collapsing to a master curve that is a straight line going through the origin [Fig. 3(f)].

One of the interesting features of the model is that if we are very close to the threshold, even though the large deviation function exists,  $W_\tau$  doesn't obey the standard fluctuation relation, as is seen in Fig. 4. Here we keep the applied force  $F = 96.0$  which is very close to the threshold value. In this case, the velocity fluctuations become non-Gaussian as is evident from the large values of Skewness ( $S$ ) and Kurtosis ( $K$ ) in Fig. 4(b). The plot of  $\ln[P(W_\tau)/P(-W_\tau)]$  vs  $W_\tau$  deviates from a straight line and if we scale  $\ln[P(W_\tau)/P(-W_\tau)]$  by  $\tau$ , even though we obtain data collapse, the master curve



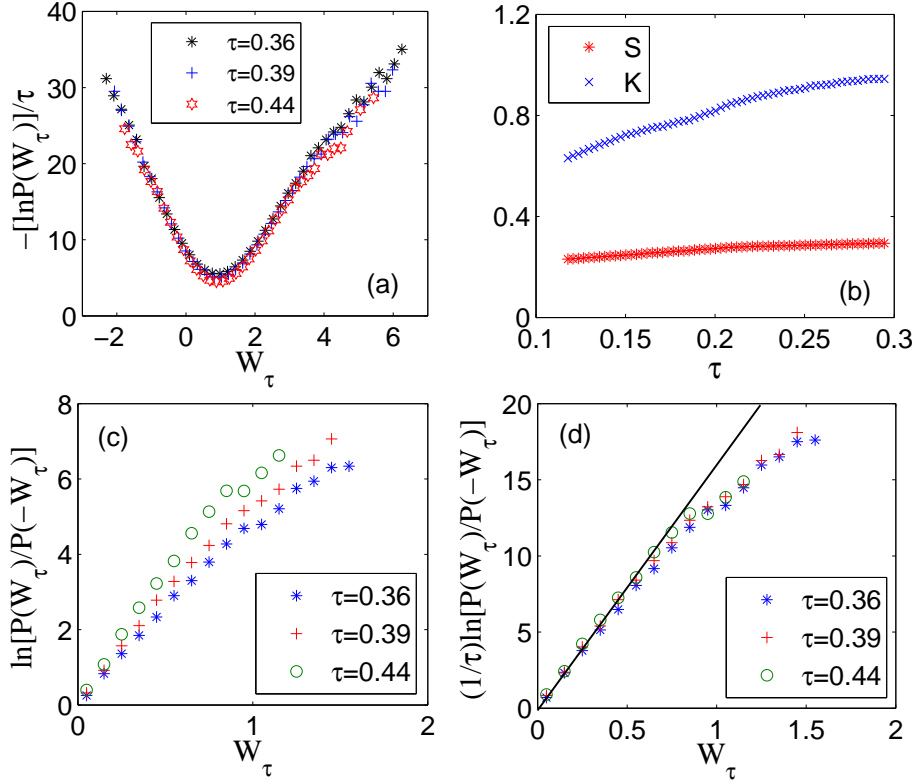


**Figure 4.** The number of springs is  $N = 200$  and  $F = 96.0$  which is very close to the threshold value. (a) The large-deviation function exists for the velocity fluctuation  $W_\tau$ . (b) The large value of  $S$  and  $K$  imply the PDF for  $W_\tau$  is non-Gaussian. (c)  $\ln[P(W_\tau)/P(-W_\tau)]$  vs  $W_\tau$  for various  $\tau$  as shown in the figure. The curves deviate from the expected straight line if FR was obeyed by  $W_\tau$ . (d) When we scale the various curves in (c) by  $\tau$ , they show excellent data collapse, but the collapsed data deviates significantly from a straight line implying the violation of the conventional FR. The straight line in the figure is just a guide to the eye.

is no longer a straight line as shown in Fig. 4(d). As long as we are very close to the threshold force, similar nonlinear FR curves are obtained even if we change the number of springs  $N$ . Our simple model thus offers an example of a system with substantial negative fluctuations and excellent data collapse consistent with the large-deviation property, but in the which the antisymmetric part of the large-deviation function is strongly nonlinear.

However, if we move slightly away from the threshold but still within the jammed state, the velocity fluctuation remains non-Gaussian, but the fluctuation relation is obeyed over the entire range of our data (Fig. 5). This shows that the source of deviation from the fluctuation relations is not merely the non-Gaussian nature of the velocity fluctuations, but it is an intrinsic nature of the model and stems from a complex mechanism near the threshold. We do not completely understand the origin of such behaviour, but further work in this direction should elucidate this very interesting phenomenon.

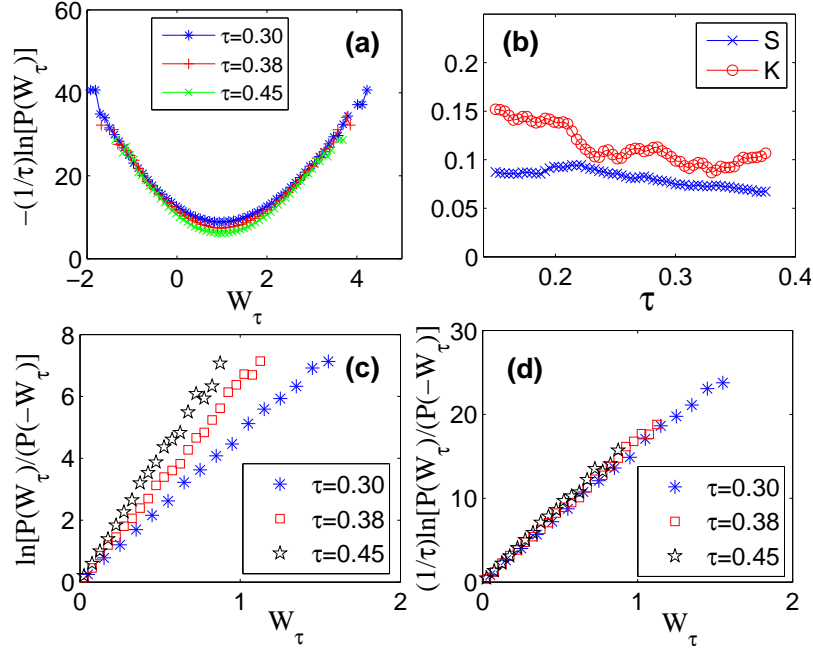


**Figure 5.** The number of springs is  $N = 200$  and applied force  $F = 86$  which is close to the threshold value. (a) The large deviation function exists. (b) The non-zero value of  $S$  and  $K$  imply that the PDF of velocity fluctuation is non-Gaussian. (c) Plot of  $\ln[P(W_\tau)/P(-W_\tau)]$  vs  $W_\tau$  for various  $\tau$  as shown in the figure. (d) When we scale  $\ln[P(W_\tau)/P(-W_\tau)]$  with  $\tau$ , the curves show data collapse and the master curve is a straight line going through the origin ascertaining the validity of FR.

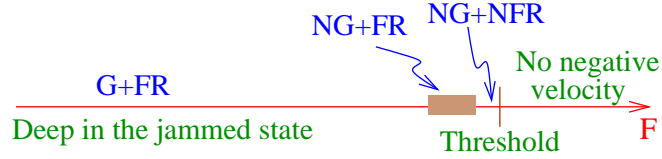


**Figure 6.** For a certain number of springs, the system goes from a jammed creeping state at low external force ( $F$ ) to a free flowing regime as  $F$  is increased. Deep in the jammed state, the PDF of velocity fluctuation is Gaussian (G) and they obey FR. However, as we increase  $F$  towards the transition, close to the transition, PDF becomes non-Gaussian (NG) although FR is still obeyed. Very close to the threshold, the PDF is NG and FR doesn't hold anymore. We do not see any negative velocity events beyond the threshold.

Let us summarize the behaviour of the model in a schematic phase diagram, Fig. 6. Deep in the jammed state, the velocity fluctuations are Gaussian (G) and they obey the fluctuation relations (FR). Near the threshold force of the jammed-to-flowing transition, the velocity fluctuations become non-Gaussian (NG) but they still obey FR. As we approach the transition, very close to the threshold, the non-Gaussian nature of the velocity fluctuation remains but they no longer obey FR. We note that these features of our model are similar to the statistical properties of entropy-consuming fluctuations

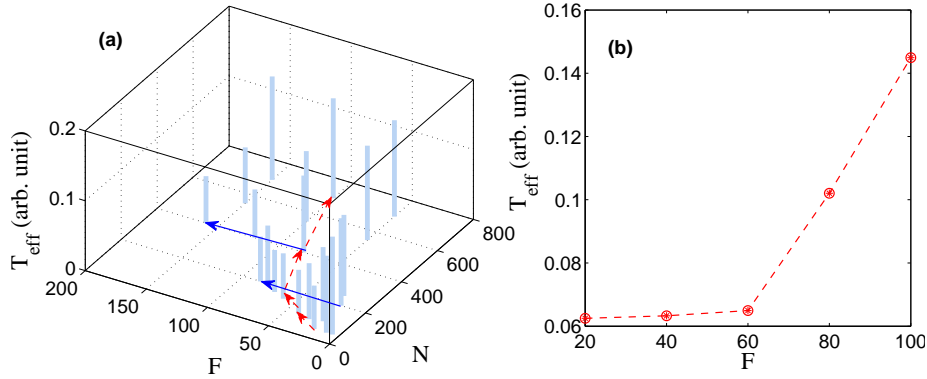


**Figure 7.** (a) The effective temperature  $T_{eff}$  extracted from Eq. (2) in arbitrary unit is plotted as a function of  $N$  and  $F$ . If we keep  $N$  fixed in the simulation,  $T_{eff}$  decreases with increasing  $F$  as is found from the two paths shown in the figure by two blue solid arrows corresponding to  $N = 200$  and  $N = 400$ . However, if we consider a different path, one such possible path is shown by the red dotted arrow, where  $N$  increases with increasing  $F$ ,  $T_{eff}$  increases on this path. (b)  $T_{eff}$  vs  $F$  for the path denoted by the red dotted arrow in (a) is shown for clarity. The number of filaments corresponding to a particular  $F$  is listed in Table 1.

in jammed states of laponite suspensions [25].

The slope of the scaled FR plot, analogous to  $\beta$  in Eq. (2), can be thought of as the inverse of an effective temperature. In the experiment, the effective temperature ( $T_{eff}$ ) increases as  $F$  increases [10]. We have pointed out earlier that there is no reason for the number of attachment points  $N$  to remain fixed in the model. In fact, it is more reasonable that  $N$  changes with  $F$ , since large applied force can disentangle or break micelles or disrupt domains giving rise to more independent regions in the dynamics. To see the behaviour of  $T_{eff}$  as a function of  $F$  within our model, we have plotted  $T_{eff}$  as a function of both  $F$  and  $N$  (Fig. 7). Let us first see what happens if we keep  $N$  fixed. As we have shown in Fig. 7(a) for  $N = 200$  and  $N = 400$  (two solid arrows),  $T_{eff}$  decreases as  $F$  increases with constant  $N$ . This is in complete contrast to what was found in the experiment [10]. However, as  $N$  increases,  $T_{eff}$  increases. Thus, to be consistent with our model, it must be that the system moves on a path on which  $N$  changes with  $F$ . With this in mind, it is possible to identify a path in the  $3d$  space of  $(N, F, T_{eff})$  where the model reproduces the correct trend of  $T_{eff}$  vs  $F$ . One such possible path is shown by the dotted arrows in Fig. 7(a) and the corresponding  $T_{eff}$  vs  $F$  behaviours is shown in Fig. 7(b) for clarity. We also show in Table 1 the particular number of attachment points for a particular force  $F$  corresponding to this path. We emphasize that this is not the only possible path consistent with the experimental trends, and the particular path that the experiment will follow is going to depend on the microscopic details of the experiment.

F	20	40	60	80	100
N	50	100	150	400	700

**Table 1.** The number of springs  $N$  taken at a particular  $F$ 

#### 4. Discussion and conclusion

In this work we have presented a simple model to understand a particular set of experiments where it was found that the velocity (or power, since the applied force is constant) fluctuations obey the fluctuation relations. The force-dependent attachment-detachment kinetics of the springs with the plate is the main mechanism behind the observed negative velocity. When the applied force is very close to the threshold, the probability distribution function of velocity fluctuations becomes non-Gaussian and the strong departures from a conventional fluctuation relation are seen. This is especially interesting given that the large-deviation property continues to hold, and we obtain data collapse when we plot  $\ln[P(W_\tau)/P(-W_\tau)]/\tau$  as a function of  $W_\tau$ , though the master curve is not a straight line. To our knowledge, our model is the first physical example of such a violation of FRs where the LDF exists. We need more experiments and theoretical analysis to understand the origin of such a phenomenon. The observation of a linear dependence of  $\log[P(W_\tau)/P(-W_\tau)]$  over a range of  $W_\tau$  is not in itself our major finding, as a function that goes through zero will normally have a linear range. It is of greater significance (a) that the function goes through zero and has appreciable weight at negative arguments, suggesting that the model captures some of the essential physics of the experiment and (b) that we observe good data collapse even when the symmetry function departs from linearity. A worthwhile future direction will be to sample the rare events [31, 32] to improve statistics in the tail of the distribution, possibly elucidating the nature of this violation of FR.

If we keep the number of springs taking part in the dynamics fixed, the observed trend of the effective temperature as a function of applied force is opposite to what was found in the experiment. However, it is more reasonable to vary the number of springs as  $F$  changes, since larger applied force may break entanglements, rupture micelles, or disrupt adhering domains. This allows the model to reproduce the correct trend of  $T_{eff}$ .

In the model, we have allowed a simple local relaxation mechanism for the springs. One can imagine more complicated modes of relaxation, for example, we can allow the springs to redistribute forces among their neighbors:

$$\frac{df_i(t)}{dt} = (1 - s_i) \left[ -\frac{f_i(t)}{\tau_1} + \frac{-2f_i + f_{i-1} + f_{i+1}}{\tau_2} \right] + s_i V(t). \quad (18)$$

We find that the presence of such a diffusive term doesn't affect the behaviour of the model much. During the attachment-detachment kinetics, other processes that could play a role include: spatial inhomogeneity and temporal variation of spring stiffness and their modification by local stretching and release, and the interplay of micellar lengths and relaxation time with imposed stresses [33].

Finally, we expect that fluctuations near yielding in a wider class of systems could show features similar to those discussed here. We have in mind situations such as the dislocation-mediated flow of stressed crystals at non-zero temperature [34], the flow of glass through the mechanism proposed by Sausset *et al.* [35], and thermally assisted depinning in general [36]. Fluctuations that take a region from the downhill to the uphill side of a pinning barrier, which are clearly more likely to happen near yielding, where effective barriers are small, should give rise to negative-velocity events.

## Acknowledgments

SKN would like to thank Sayantan Majumdar and Sumilan Banerjee for discussions and TIFR Hyderabad for hospitality. SKN was supported in part by the University Grants Commission and SR by a J.C. Bose Fellowship from the Department of Science and Technology, India. AKS thanks CSIR for support as Bhatnagar Fellowship. BC acknowledges discussions with Peter Sollich, the hospitality of KITP, Santa Barbara where some of this work was done and support from NSF-DMR award 0905880.

- [1] Evans D J, Cohen E G D and Morris G P, 1993 *Probability of second law violations in shearing steady states. Phys. Rev. Lett.* **71** 2401
- [2] Gallavotti G and Cohen E G D, 1995 *Dynamical ensembles in non-equilibrium statistical mechanics. Phys. Rev. Lett.* **74** 2694
- [3] Gallavotti G and Cohen E G D, 1995 *Dynamical ensembles in stationary states. J. Stat. Phys.* **80** 931
- [4] Jarzynski C, 1997 *Nonequilibrium equality for free energy differences. Phys. Rev. Lett.* **78** 2690
- [5] Crooks G E, 1998 *Nonequilibrium measurements of free energy differences for microscopically reversible markovian systems. J. Stat. Phys.* **90** 1481
- [6] Bochkov G and Kuzovlev Y E, 1977 *General theory of thermal fluctuations in nonlinear systems. Sov. Phys. JETP* **45** 125
- [7] Bochkov G N and Kuzovlev Y E, 1981 *Nonlinear fluctuation-dissipation relations and stochastic models in nonequilibrium thermodynamics: I. generalized fluctuation-dissipation theorem. Physica A* **106** 443
- [8] Touchette H, 2009 *The large deviation approach to statistical mechanics. Physics Reports* **478** 1
- [9] Oono Y, 1989 *Large deviation and statistical physics. Prog. Theoret. Phys. Suppl.* **99** 165
- [10] Majumdar S and Sood A K, 2008 *Nonequilibrium fluctuation relation for sheared micellar gel in a jammed state. Phys. Rev. Lett.* **101** 078301
- [11] Wang G M, Carberry D M, Reid J C, Sevick E M and Evans D J, 2005 *Demonstration of the steady-state fluctuation theorem from a single trajectory. J. Phys.: Condens. Matter* **17** S3239
- [12] Evans D J and Searles D J, 2002 *The fluctuation theorem. Adv. Phys.* **51** 1529
- [13] Douarche F, Joubaud S, Garnier N B, Petrosyan A and Ciliberto S, 2006 *Work fluctuation theorems for harmonic oscillators. Phys. Rev. Lett.* **97** 140603
- [14] Kumar N, Ramaswamy S and Sood A K, 2011 *Symmetry properties of the large-deviation function of the velocity of a self-propelled polar particle. Phys. Rev. Lett.* **106** 118001
- [15] Gomez-Solano J R, Petrosyan A and Ciliberto S, 2011 *Heat fluctuations in a nonequilibrium bath. Phys. Rev. Lett.* **106** 200602
- [16] Gradenigo G, Puglisi A, Sarracino A and Marconi U M B, 2012 *Nonequilibrium fluctuations in a driven stochastic lorentz gas. Phys. Rev. E* **85** 031112

- [17] Sabhapandit S, 2011 *Work fluctuations for a harmonic oscillator driven by an external random force.* *Euro. Phys. Lett.* **96** 20005
- [18] van Zon R and Cohen E G D, 2003 *Stationary and transient work-fluctuation theorems for a dragged brownian particle.* *Phys. Rev. E* **67** 046102
- [19] Chatterjee D and Cherayil B J, 2010 *Exact path-integral evaluation of the heat distribution function of a trapped brownian oscillator.* *Phys. Rev. E* **82** 051104
- [20] Chatterjee D and Cherayil B J, 2011 *Single-molecule thermodynamics: the heat distribution function of a charged particle in a static magnetic eld.* *J. Stat. Mech.* P03010
- [21] Ciliberto S, Joubaud S and Petrosyan A, 2010 *Fluctuations in out-of-equilibrium systems: from theory to experiment.* *J. Stat. Mech.* P12003
- [22] Cugliandolo L F, 2011 *The effective temperature.* *J. Phys. A: Math. Theor.* **44** 483001
- [23] van Zon R and Cohen E D, 2003 *Extension of the fluctuation theorem.* *Phys. Rev. Lett.* **91** 110601
- [24] Touchette H and Cohen E G D, 2007 *Fluctuation relation for a lévy particle.* *Phys. Rev. E* **76** 020101(R)
- [25] Majumdar S and Sood A K, 2012 *Statistical properties of entropy-consuming fluctuations in jammed states of laponite suspensions: Fluctuation relations and generalized gumbel distribution.* *Phys. Rev. E* **85** 041404
- [26] Chechkin A V and Klages R, 2009 *Fluctuation relations for anomalous dynamics.* *J. Stat. Mech.* L03002
- [27] Sollich P, Lequeux F, Hébraud P and Cates M E, 1997 *Rheology of soft glassy materials.* *Phys. Rev. Lett.* **78** 2020
- [28] Sollich P, 1998 *Rheological constitutive equation for a model of soft glassy materials.* *Phys. Rev. E* **58** 738
- [29] Fielding S M, Cates M E and Sollich P, 2000 *Aging and rheology in soft materials.* *J. Rheol.* **44** 323
- [30] Voter A F, 2005 *Introduction to the kinetic monte carlo method.* In Sickafus K E and Kotomin E A, editors, *Radiation Effects in Solids.* Springer, NATO Publishing Unit, Dordrecht, The Netherlands
- [31] Berryman J T and Schilling T, 2010 *Sampling rare events in nonequilibrium and nonstationary systems.* *J. Chem. Phys.* **133** 244101
- [32] Kundu A, Sabhapandit S and Dhar A, 2011 *Application of importance sampling to the computation of large deviations in nonequilibrium processes.* *Phys. Rev. E* **83** 031119
- [33] Kumar N, Majumdar S, Sood A, Govindarajan R, Ramaswamy S and Sood A, 2012 *Oscillatory settling in wormlike-micelle solutions: bursts and a long time scale.* *Soft Matter* **8** 4310
- [34] Zippelius A, Halperin B I and Nelson D R, 1980 *Dynamics of two-dimensional melting.* *Phys. Rev. B* **22** 2514
- [35] Sausset F, Biroli G and Kurchan J, 2010 *Do solids flow?* *J. Stat. Phys.* **140** 718
- [36] Bustingorry S, Kolton A B and Giamarchi T, 2012. *Thermal rounding exponent of the depinning transition of an elastic string in a random medium.* arXiv: 1204.0772